Adaptive Control Strategy for VSC-Based Systems Under Unbalanced Network Conditions

Andres E. Leon, *Student Member, IEEE*, Juan M. Mauricio, *Member, IEEE*, Jorge A. Solsona, *Senior Member, IEEE*, and Antonio Gómez-Expósito, *Fellow, IEEE*

***Abstract*—A new adaptive control strategy, intended to improve the ride-through capability of high-voltage direct current (HVDC) systems under unbalanced network conditions and parameter uncertainties, is introduced. The proposed strategy resorts to a model reference adaptive control plus a resonant filter. The resonant filter scheme is based on a unique synchronous reference frame that prevents the use of the customary sequence component detector, increasing the controller bandwidth accordingly. Several tests are conducted to compare the proposed scheme against existing HVDC controllers, showing an improved performance regarding: 1) elimination of the 2ω ripple on the dc voltage arising during ac-side imbalances; 2) accurate and decoupled active and reactive power tracking when converter parameters are not perfectly known.**

***Index Terms*—DC voltage control, imbalance and parameter uncertainties, nonlinear adaptive control, power flow control, resonant controller, voltage source converter (VSC), VSC-based high-voltage direct current (HVDC) systems.**

I. Introduction

HIGH-VOLTAGE direct current (HVDC) systems based on voltage source converters (VSC-HVDC) constitute a promising technology currently being developed by companies such as ABB and Siemens [1], [2]. A notable increase in the power transmission capability of these systems is making the VSC-HVDC technology an attractive alternative to the traditional ac transmission systems [3]. Conventional HVDC systems employ line commutated, current-source converters requiring a synchronous voltage source in order to operate. The conversion process demands reactive power from filters, shunt banks, or capacitors which are part of the converter station. Any surplus or deficit in reactive power must be accommodated by the ac system. The VSC-HVDC technology, lacking this limitation, offers added advantages associated with the possibility of independently controlling the active and reactive power. Also, its fast transient response when controlling the ac current components makes this technology very interesting not only for subtransmission but also for distribution systems. The increasing number of current and future areas where VSC-HVDC systems can play a key role, further focuses the spotlight on this technology. Among them, the following can be cited: small and isolated remote loads, power supply to islands, express infeed systems to city centers, improving power quality and power flows in distribution systems, remote small-scale generation, offshore wind farms, deep-sea crossings, and multiterminal systems [4].

In future power systems, several new sources of electricity generation must be embedded. Distributed generation is going to change the current operation philosophy of distribution and, to a certain extent, subtransmission power grids. Furthermore, hybrid (HEV) and electrical vehicles (EV) or energy storage systems (ESS) will have to be fed. Most of these elements need an interface for them to be connected to the ac power grid, which could be simplified in the case of having a dc power network in their vicinity. This approach is shown in Fig. 1 where HEV, EV, ESS, solar panels (PV), wind energy conversion systems (WECS) and other ac/dc networks are considered. In order to avoid possible interactions among all these elements, when connected to the same dc bus, the dc voltage control should be as fast and tight as possible. Therefore, strategies for controlling ac currents and dc voltage must be efficient at tracking references and rejecting disturbances. For example, it would be desirable for the control strategy to avoid the characteristic double frequency ripple on the dc voltage under ac unbalanced conditions.

This paper deals with the design of suitable controllers for VSC-based HVDC systems, arising in the upcoming context described above. A new adaptive control strategy for improving the ride-through capability of HVDC systems, under both unbalanced network conditions and parameter variations, is presented. The proposed scheme is based on a model reference adaptive control plus a resonant filter, which does not rely on a sequence component separator. This results in a controller with an extended bandwidth, capable of accurately controlling the reactive power exchanged with the grid and eliminating the 2ω ripple on the dc voltage.

The paper is organized as follows. A background of techniques for controlling VSC and HVDC systems is developed in Section II. In Section III the VSC-based HVDC model is presented. Then, Section IV describes the calculation of reference currents required to eliminate the double-frequency ripple on the dc voltage under unbalanced conditions and to control the reactive power at the converter station terminals. In Section V the adaptive plus resonant controller is introduced in order to obtain a high-performance HVDC system during both unbalanced

Manuscript received November 26, 2009; revised July 13, 2010; accepted September 08, 2010. Date of current version November 19, 2010. This work was supported in part by Universidad Nacional del Sur, Consejo Nacional de Investigaciones Científicas y Técnicas (CONICET) and Agencia Nacional de Promoción Científica y Tecnológica (ANPCyT), Argentina, and in part by the Spanish Ministry of Education and Science (MEC) under Grant ENE-2007-68032-C04-02 and Junta de Andalucía under Grant and TEP-5170. Paper no. TSG-00023-2009.

A. E. Leon and J. A. Solsona are with Instituto de Investigaciones en Ingeniería Eléctrica (IIIE) "Alfredo Desages" (UNS-CONICET), Departamento de Ingeniería Eléctrica y de Computadoras, Universidad Nacional del Sur (UNS), Bahía Blanca, Argentina (e-mail: aleon@ymail.com; jsolsona@uns.edu.ar).

J. M. Mauricio and A. Gómez-Expósito are with the Department of Electrical Engineering, University of Seville, 41092 Seville, Spain. (e-mail: j.m.mauricio@ieee.org; age@us.es).

Digital Object Identifier 10.1109/TSG.2010.2076840

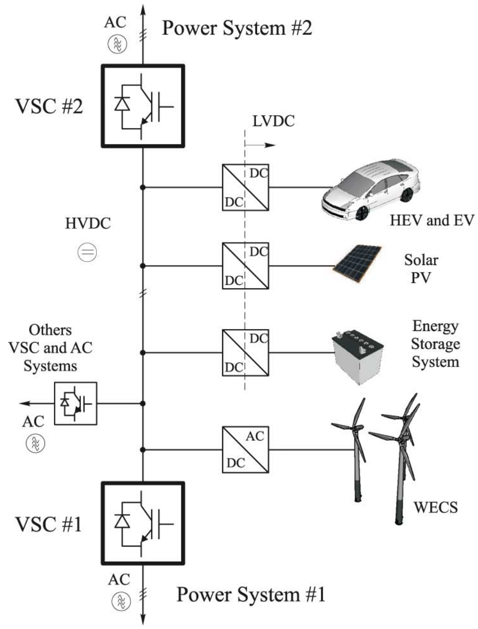

Fig. 1. Layout of the new trend in distributed generation systems.

faults and parameter uncertainties. Performance tests, discussions and results are shown in Section VI. Finally, conclusions are given in Section VII.

II. Background

A. State of the Art on VSC Control Under Unbalanced Conditions

In the last decade several works have addressed the problem of controlling VSCs under unbalanced conditions. Most of them can be classified in the following two categories:

The first approach, based on a dual sequence control (DSC) scheme [5]–[12], independently controls the positive and negative sequences using two reference frames rotating at synchronous speed but in opposite directions. They are easily tuned by means of appropriate PI controllers, because each frame deals with separate dc signals. However, they are based on a sequence component detector that reduces the bandwidth of the controller.

The second category of methods tries to overcome the above shortcoming by removing the sequence separation. This is achieved by using proportional plus resonant (PR) controllers [13]–[20] which allow tracking, without steady state error, constant and sinusoidal current references, arising under unbalanced conditions.

Stability and performance of the above-mentioned controllers are affected by parameter variations of the VSC components. The parameters of the coupling reactor or transformer, such as the inductance and resistance, filter inductors, and connection cables are frequency dependent. Moreover, some of those parameters vary with temperature effects, core saturation, minor internal faults or changes, aging of components, cable overload, and other environmental conditions. For this reason, some authors propose in the literature the use of adaptive controllers in order to maintain the performance even under varying parameter conditions.

For example, in [21]–[24] adaptive controllers are presented, but unbalanced conditions are not taken into account. On the other hand, several control strategies intended for unbalanced conditions are presented in [5]–[10], [13]–[17], [25]–[29], but they lack of adaptive features when VSC parameters vary. The works presented in [18]–[20], [30] consider both an adaptive behavior and unbalanced conditions. Nevertheless, those approaches are not designed to eliminate the double-frequency ripple appearing on the VSC dc bus under unbalanced conditions, which is an important requirement for VSC-HVDC applications, as explained below.

B. 2ω-Ripple Elimination Techniques

In this paper, the VSC controller focuses specifically on HVDC systems. For this reason, the way in which the control strategy deals with the double-frequency ripple appearing on the dc voltage under unbalanced conditions is very important. In some applications the 2ω ripple is maintained on purpose in order to accomplish other objectives, for example not to inject negative-sequence current or to achieve a balanced voltage at the Point of Common Coupling (PCC) when an unbalanced condition arises in the network, as in references [13], [18]–[20], [25], [27], [29], [30]. However, in HVDC systems it is preferred to keep a constant voltage in the dc line in spite of unbalanced conditions on the ac side. There are four techniques for eliminating the 2ω oscillations of the dc voltage under unbalanced conditions.

▷ The first one obtains the positive- and negative-sequence current references by nullifying the oscillating active power and the reactive power at the PCC [7], [28]. The drawback of this method, when the coupling reactance is not negligible, is that the oscillating active power is not null at the VSC inner terminal, as required for a proper elimination of the 2ω ripple.

▷ The second technique cancels out the oscillating active power and the reactive power at the converter inner terminal [5]. Although the dc voltage oscillations are completely eliminated, the unity power factor condition is not accomplished at the PCC, as desired.

▷ The third method eliminates the 2ω oscillation on the dc voltage and achieves a unity power factor at the PCC, by nullifying the oscillating active power at the converter inner terminal and the reactive power at the PCC [8]–[10]. However, this technique needs to solve a nonlinear equation system and the accurate reactance value is also required.

▷ Finally, the fourth method shares the same benefits as the third one but, as will be explained in Section III, by using the converter internal voltages the reactance value is not needed and a linear equation system is obtained in order to calculate the positive- and negative-sequence current references [15]–[17].

C. HVDC System Controllers

The above-mentioned strategies are intended for isolated VSCs or STATic COMpensators (STATCOM) applications. When the bibliography is looked specifically for HVDC-related systems, several approaches can be found considering

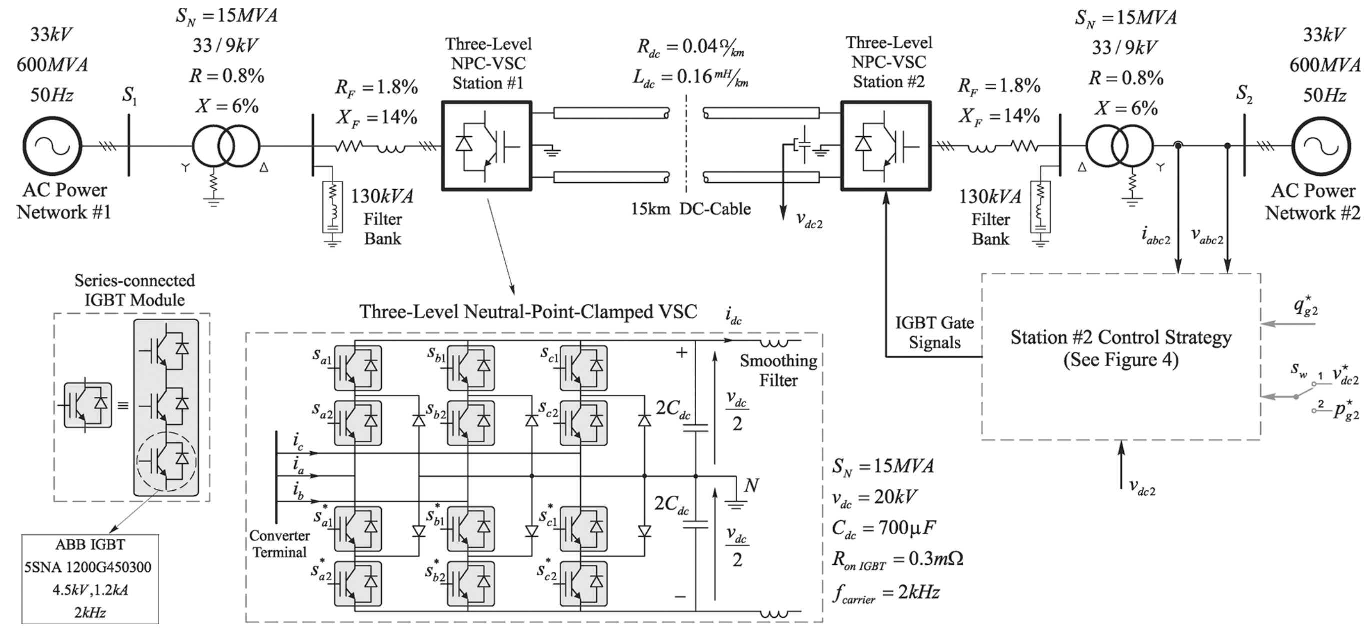

Fig. 2. Data and parameters of the VSC-based HVDC transmission system.

either adaptive behavior or unbalanced conditions. In some of them [31]–[39] neither unbalanced conditions nor an adaptive characteristic are taken into account. In [40]–[44], an approach capable of adapting to HVDC parameter variation is presented, but the adaptive controller is not designed to ride through unbalanced network conditions. On the other hand, the controllers in [45]–[50] try to improve the HVDC performance under unbalanced conditions but the adaptive behavior when parameter variations occur is not addressed. For this reason, an adaptive control strategy, intended to improve the ride-through capability of HVDC systems under unbalanced network conditions and parameter uncertainties, is introduced in this paper.

III. HVDC System Model

The power system considered is a HVDC system in which two VSCs are linked by a 15-km dc cable. System data and parameters are shown in Fig. 2. Both converter stations are composed of three-level neutral-point-clamped (NPC) VSCs, connected through step-up transformers and filter inductors to the distribution grid. They employ insulated-gate bipolar transistors (IGBTs) and the valve switching scheme follows a pulsewidth modulation (PWM) pattern. The VSC model for the converter stations in a $d-q$ synchronous reference frame is given by [34], [35]

$$\frac{1}{\Omega_B} L\dot{i}_d = -Ri_d - L\omega i_q - e_d + v_d, \quad (1)$$

$$\frac{1}{\Omega_B} L\dot{i}_q = -Ri_q + L\omega i_d - e_q + v_q, \quad (2)$$

$$\frac{1}{\Omega_B} C_{\rm dc}\dot{v}_{\rm dc} = \frac{3}{2}\left(\eta_d i_d + \eta_q i_q\right) - \frac{v_{\rm dc}}{R_L} - i_{\rm dc} \quad (3)$$

where the converter internal voltages are defined as

$$e_d \triangleq \eta_d v_{\rm dc}, \quad (4)$$

$$e_q \triangleq \eta_q v_{\rm dc} \quad (5)$$

TABLE I
NOMENCLATURE

Variables and parameters	
i_d, i_q	dq-axes VSC currents [pu]
v_d, v_q	dq-axes network voltages (at the PCC) [pu]
e_d, e_q	dq-axes converter internal voltages (at the converter inner terminal) [pu]
η_d, η_q	dq control inputs of the VSC
v_{dc}	DC-link voltage [pu]
i_{dc}	DC-link current [pu]
Ω_B	Network angular frequency ($2\pi \times 50$ Hz) [rad/s]
ω	Network angular frequency [pu]
R, L	VSC coupling resistance and inductance [pu]
R_L	Equivalent resistance of the converter losses [pu]
C_{dc}	DC-link capacitance [pu]
p	Instantaneous active power
q	Instantaneous reactive power
s_g	Apparent power at the PCC
s_t	Apparent power at the converter inner terminal
Superscripts	
$+$, $-$	Positive and negative sequence
$\star$	Reference value
d	Desired reference value
$\hat{}$	Estimated value
$*$	Conjugate
Subscripts	
d, q	d- and q-axis component
g	VSC input magnitude
t	converter inner terminal magnitude

and all states and parameters are in a per unit system on a 15-MVA base. The nomenclature adopted is described in Table I. The instantaneous vectors of current, grid voltage, and converter internal voltage in a $d-q$ synchronous reference frame are defined as $\mathbf{i}_{\rm dq} = i_q + ji_d$, $\mathbf{v}_{\rm dq} = v_q + jv_d$ and $\mathbf{e}_{\rm dq} = e_q + je_d$, respectively.

IV. Reference Current Calculation

This section describes how to obtain the positive- and negative-sequence reference currents under unbalanced ac network conditions. The technique below presents as advantages: 1) reference currents are computed from a linear equation system, and

2) it does not need the knowledge of the coupling filter or transformer reactance.

The apparent power from the grid is given by [7], [10]

$$\begin{aligned} s_g &= \mathbf{v}_{\text{abc}}\mathbf{i}_{\text{abc}}^*, \\ &= \frac{3}{2}(\mathbf{v}_{\text{dq}}^+ e^{j\omega t} + \mathbf{v}_{\text{dq}}^- e^{-j\omega t})(\mathbf{i}_{\text{dq}}^+ e^{j\omega t} + \mathbf{i}_{\text{dq}}^- e^{-j\omega t})^*, \\ &= (p_g + p_{\text{gs}} \sin 2\omega + p_{\text{gc}} \cos 2\omega) \\ &\quad + j(q_g + q_{\text{gs}} \sin 2\omega + q_{\text{gc}} \cos 2\omega) \end{aligned} \tag{6}$$

where p_g and q_g are the constant active and reactive power, whereas p_{gs}, p_{gc}, q_{gs} and q_{gc} are the sine and cosine 2ω oscillation terms of the active and reactive power, respectively. Likewise, the apparent power at the converter terminal can be written as

$$\begin{aligned} s_t &= \mathbf{e}_{\text{abc}}\mathbf{i}_{\text{abc}}^*, \\ &= \frac{3}{2}(\mathbf{e}_{\text{dq}}^+ e^{j\omega t} + \mathbf{e}_{\text{dq}}^- e^{-j\omega t})(\mathbf{i}_{\text{dq}}^+ e^{j\omega t} + \mathbf{i}_{\text{dq}}^- e^{-j\omega t})^*, \\ &= (p_t + p_{\text{ts}} \sin 2\omega + p_{\text{tc}} \cos 2\omega) \\ &\quad + j(q_t + q_{\text{ts}} \sin 2\omega + q_{\text{tc}} \cos 2\omega) \end{aligned} \tag{7}$$

where the same definitions of constant and oscillating power terms apply here. Expanding (6) and (7), the relations below are obtained:

$$\frac{2}{3}p_g = i_d^- v_d^- + i_d^+ v_d^+ + i_q^- v_q^- + i_q^+ v_q^+, \tag{8}$$
$$\frac{2}{3}q_g = i_q^- v_d^- + i_q^+ v_d^+ - i_d^- v_q^- - i_d^+ v_q^+, \tag{9}$$
$$\frac{2}{3}p_{\text{ts}} = i_q^+ e_d^- - i_q^- e_d^+ - i_d^+ e_q^- + i_d^- e_q^+, \tag{10}$$
$$\frac{2}{3}p_{\text{tc}} = i_d^+ e_d^- + i_d^- e_d^+ + i_q^+ e_q^- + i_q^- e_q^+. \tag{11}$$

In order to eliminate the 2ω ripple on the dc voltage the oscillating active power at the converter terminal must be zeroed $(p_{\text{ts}} = p_{\text{tc}} = 0)$. Besides, the values of p_g and q_g must be set to control the active and reactive power injected to the grid by the converter station. Finally, taking into account these considerations, from the linear equation system (8)–(11), the reference currents are obtained as

$$\begin{bmatrix} i_d^{+\star} \\ i_q^{+\star} \\ i_d^{-\star} \\ i_q^{-\star} \end{bmatrix} = \frac{2}{3} \begin{bmatrix} v_d^+ & v_q^+ & v_d^- & v_q^- \\ -v_q^+ & v_d^+ & -v_q^- & v_d^- \\ -e_q^- & e_d^- & e_q^+ & -e_d^+ \\ e_d^- & e_q^- & e_d^+ & e_q^+ \end{bmatrix}^{-1} \begin{bmatrix} p_g^\star \\ q_g^\star \\ 0 \\ 0 \end{bmatrix}. \tag{12}$$

V. Adaptive Plus Resonant Controller for the HVDC Converter Station

A. *Converter Station #1 Controller*

The equations modeling the dynamics of the converter currents are (1) and (2). They can be rewritten in a matrix form as

$$\dot{\mathbf{x}} = \Omega_B \begin{bmatrix} -\frac{R}{L} & -1 \\ 1 & -\frac{R}{L} \end{bmatrix} \mathbf{x} + \frac{1}{L}\mathbf{u} \tag{13}$$

where

$$\mathbf{x} \triangleq [x_1 \quad x_2]^T = [i_d \quad i_q]^T, \tag{14}$$

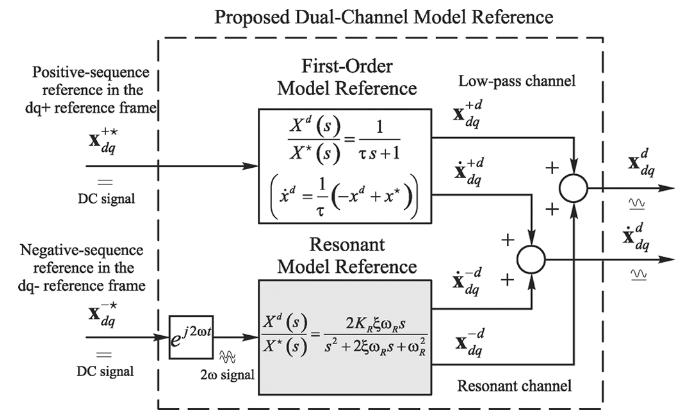

Fig. 3. Proposed dual-channel model reference.

$$\mathbf{u} \triangleq [u_1 \quad u_2]^T = \Omega_B [v_d - \eta_d v_{\text{dc}} \quad v_q - \eta_q v_{\text{dc}}]^T. \tag{15}$$

The model reference adaptive control (MRAC) built in this section requires that a model reference be introduced to obtain the desired reference values and its time derivatives. As the control scheme is in a positive synchronous reference frame, both constant and sinusoidal signals must be tracked at the same time. For this reason, the dual-channel model reference of Fig. 3, comprising a first-order and a resonant filter, is adopted in this work. From the inputs provided by (12), the desired reference values $(\mathbf{x}^d)$ and its time derivatives $(\dot{\mathbf{x}}^d)$, needed in the following control stage, are obtained.

Since the relative degree of i_d and i_q is one, a first-order tracking error dynamics is chosen

$$\dot{\mathbf{e}} + a_d \mathbf{e} = \mathbf{0} \tag{16}$$

where the tracking error is defined as $\mathbf{e} = [e_1 \quad e_2] \triangleq \mathbf{x} - \mathbf{x}^d$, and a_d is a design constant value. From the error dynamics (16) and taking into account (13), the auxiliary control input can be obtained as

$$\mathbf{u} = \Omega_B \begin{bmatrix} R & L \\ -L & R \end{bmatrix} \mathbf{x} + L(\dot{\mathbf{x}}^d - a_d \mathbf{e}). \tag{17}$$

Up to this point, the control law (17) would be the same as if feedback linearization, or any other technique canceling the coupling between d and q axes, had been applied. However, as mentioned in the introduction, changes or mismatches in the VSC parameters can occur, in which case this kind of control laws could see its performance very degraded, because of an imperfect coupling cancelation. Consequently, a control law analogous to (17) is proposed, where the estimated values of resistance $(\hat{R})$ and inductance $(\hat{L})$ come from an adaptation law. Therefore,

$$\mathbf{u} = \Omega_B \begin{bmatrix} \hat{R} & \hat{L} \\ -\hat{L} & \hat{R} \end{bmatrix} \mathbf{x} + \hat{L}(\dot{\mathbf{x}}^d - a_d \mathbf{e}). \tag{18}$$

By expanding (18) and considering (15) the control signals for the converter station are obtained

$$\eta_d = \frac{1}{v_{\text{dc}}} \left(v_d - \hat{R}x_1 - \hat{L}x_2 - \frac{\hat{L}}{\Omega_B} \left(\dot{x}_1^d - a_d e_1 \right) \right), \tag{19}$$

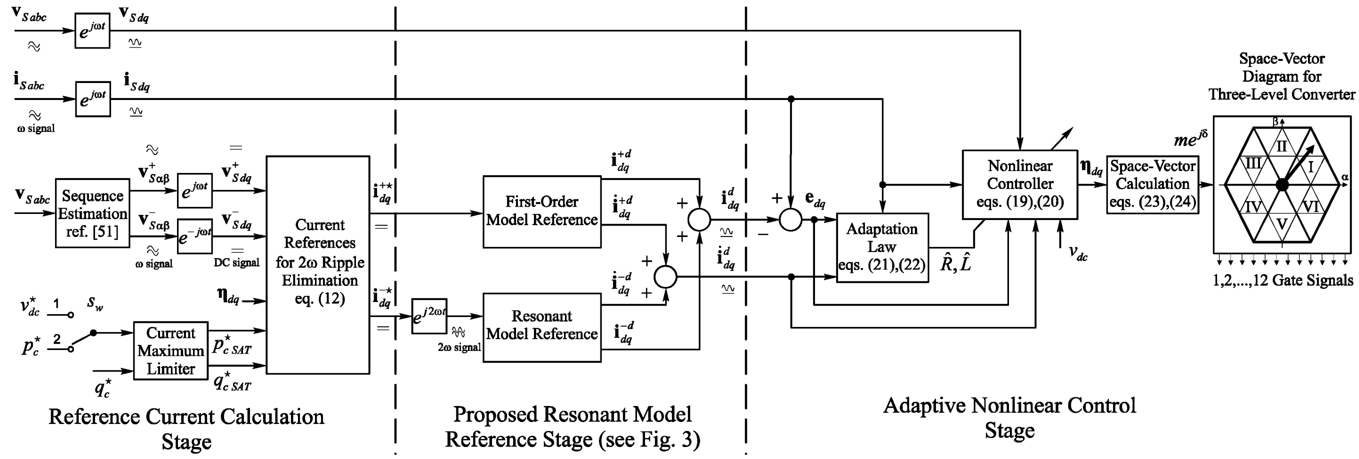

Fig. 4. Current reference calculation and control strategy stages.

$$\eta_q = \frac{1}{v_{\rm dc}}\left(v_q - \hat{R}x_2 + \hat{L}x_1 - \frac{\hat{L}}{\Omega_B}\left(\dot{x}_2^d - a_d e_2\right)\right) \quad (20)$$

where the following adaptation law is proposed to obtain the estimated VSC parameters:

$$\dot{\hat{R}} = -\gamma\Omega_B(e_1x_1 + e_2x_2), \quad (21)$$

$$\dot{\hat{L}} = -\gamma\left(\Omega_B(e_1x_2 - e_2x_1) + e_1\left(\dot{x}_1^d - a_d e_1\right) + e_2\left(\dot{x}_2^d - a_d e_2\right)\right). \quad (22)$$

Details of the adaptation law derivation along with its stability proof are included in the Appendix.

The actual driving signals for the VSC are obtained via a pulsewidth modulator (PWM) with inputs η_d and η_q [see (19) and (20)]. The amplitude and phase required for the space-vector modulation (SVM) stage are calculated as

$$m = \sqrt{\eta_d^2 + \eta_q^2}, \quad (23)$$

$$\delta = \arctan(\eta_d, \eta_q). \quad (24)$$

A block diagram representing the proposed adaptive plus resonant nonlinear controller is shown in Fig. 4.

B. Converter Station #2 Controller

The converter station #2 controller is almost the same as the one developed in the above subsection for the station #1. The difference is that the active power reference $p_g^\star$ is managed by a dc voltage control loop. In this way, the active power of the station #2 is used for maintaining a constant dc voltage, closing the active power balance transmitted by the HVDC system. The dc voltage control loop is implemented via a PI loop as follows:

$$p_{g2}^\star = k_{\rm dcp}(v_{\rm dc2} - v_{\rm dc2}^\star) + k_{\rm dci}\int(v_{\rm dc2} - v_{\rm dc2}^\star)dt + p_{g1} \quad (25)$$

where a feedforward term from the active power injected by the converter station #1 (p_{g1}) is included in order to minimize the dc voltage variations when active power transients occur. Besides, as in the station #1, the reactive power consumed or injected by the station #2 (q_{g2}) can be independently controlled to fulfil grid code requirements or to support ac network voltages.

VI. Performance Testing

This section presents the most relevant test results regarding the assessment of the proposed control strategy. The HVDC system, VSCs, and control strategies are implemented on realistic models (discrete switching devices) by using the SimPowerSystems blockset of MATLAB. Controller gains are set to: $a_d = 400$, $\gamma = 0.4$, $\tau = 2.5$ ms, $K_R = 1$, $\omega_R = 2\pi \times 100$, $\xi = 0.477$, $k_{\rm dcp} = 4000$, and $k_{\rm dci} = 80 \times 10^3$. The power system configuration and parameters used in the tests are shown in Fig. 2.

A. Step Tracking and Adaptive Behavior Under Balanced Conditions

The first test shows how the proposed control strategy behaves when tracking power steps. The ability to adapt the VSC parameters is also confirmed by setting the initial estimates of converter parameters to zero (i.e., no parameter information is provided in the controller startup). In Fig. 5(a), (b), (c), and (d) the actual (solid line) and reference (dashed line) active and reactive powers are shown. A fast and decoupled step tracking can be observed, except for the first step, when a small coupling can be noticed as a consequence of the adaptation time taken by the controller to estimate the actual converter parameters. Fig. 5(e) shows the dc voltages in both converter stations. As can be seen, only small deviations of the reference voltage $(v_{\rm dc2}^\star)$ occur in the rectifier station (converter station #2), taking into account the large power variations imposed. The difference in $v_{\rm dc1}$ and $v_{\rm dc2}$ dc voltages allows the active power to flow between converter stations. Finally, in Fig. 5(f) the actual VSC parameters and those estimated by the proposed adaptive strategy are shown. A quick and accurate estimation is accomplished by the proposed adaptation mechanism.

A second test is presented in order to compare the proposed adaptive PR controller against a conventional nonadaptive PR controller when a 20% mismatch exists between the actual and assumed VSC coupling impedance. Fig. 6(a) and (b) show the performance of the proposed controller when several active and

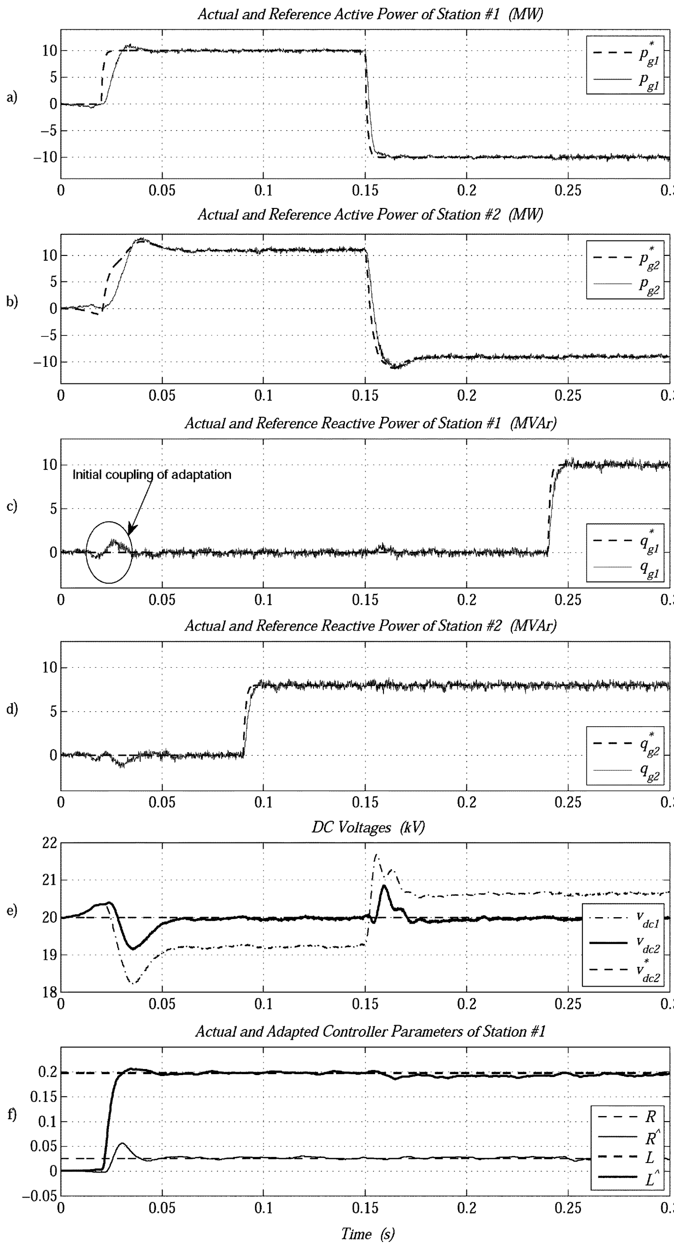

Fig. 5. Behavior of the proposed controller when tracking power steps without any converter parameter knowledge.

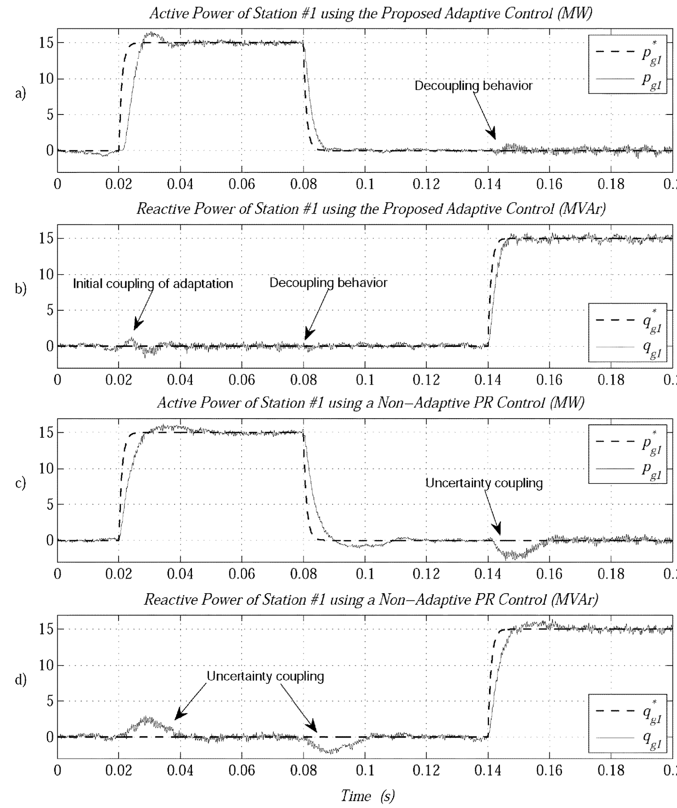

Fig. 6. Performance of the proposed adaptive controller versus a nonadaptive PR control scheme for a 20% mismatch between actual and assumed VSC impedance.

reactive power steps are introduced. Again, an accurate and decoupled tracking of power is accomplished. On the other hand, in Fig. 6(c) and (d), it is observed that the conventional nonadaptive PR controller can not completely decouple the active and reactive powers, as parameter mismatches prevent a perfect cancelation of the converter model coupling. This stresses the importance of resorting to an adaptive characteristic in realistic converter applications when high performance is required.

B. Asymmetrical Fault Test and Elimination of the DC Voltage Ripple

In this last test, the asymmetrical fault ride-through capability of the proposed control strategy is assessed. Three controllers are compared, namely: *i)* a control scheme that, under unbalanced conditions, tries to cancel the negative-sequence current rather than the 2ω ripple on the dc voltage; *ii)* a conventional nonadaptive PR controller which eliminates the 2ω oscillations; and *iii)* the proposed adaptive controller.

The performed test consists of a two-phase fault taking place at the S_1-bus (converter station #1, see Fig. 2). In order to test the robustness of each control strategy a 20% mismatch between the controller and the actual converter impedance is considered. In Fig. 7(a) the high imbalance of the S_1-bus ac voltage, due to the asymmetrical fault, is clearly seen. In Fig. 7(b) the dc voltage regulation with the controller *i)* is shown. As this sort of controller is not designed to eliminate the 2ω ripple, a big oscillation arises during the fault time. In Fig. 7(c) the performance of the controller *ii)* is presented. This kind of controller is capable of eliminating the 2ω oscillations on the dc voltage, provided the actual converter parameters are perfectly known. When there exists some mismatch between the controller and the actual converter parameters, a 2ω ripple still remains on the dc bus. Fig. 7(d) shows the dc voltage behavior when the proposed adaptive controller is implemented. In this case, the dc voltage is both well regulated and without the 2ω oscillations, in spite of the high unbalanced ac voltages and the uncertainties in the converter parameters. Also, the absence of the 2ω-ripple on the dc-side voltage eliminates odd harmonics in the ac-side currents.

VII. Conclusion

A new control strategy for VSC-based HVDC systems is presented in this paper. The proposed strategy, based on a model reference adaptive control plus a resonant filter, achieves

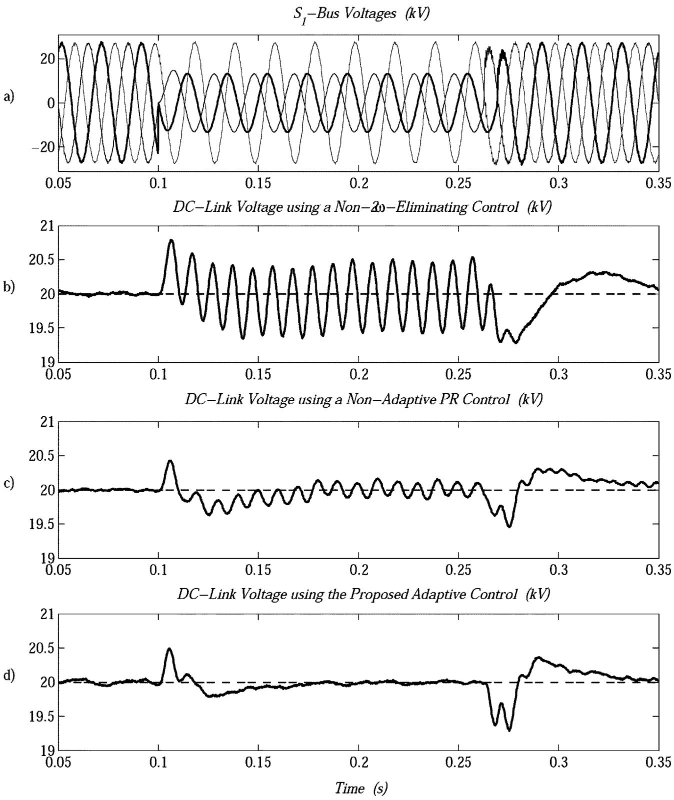

Fig. 7. Asymmetrical fault test and comparison of the 2ω ripple elimination with the proposed technique against conventional controllers.

an excellent performance of HVDC systems under both unbalanced network conditions and parameter variations, enhancing the symmetrical and asymmetrical ride-through capability of such devices. Furthermore, the proposed controller eliminates the 2ω ripple on the dc voltage during network imbalances and accomplishes an accurate and decoupled active and reactive power tracking capability. The resonant filter scheme, based on a unique positive-sequence synchronous reference frame, increases the controller bandwidth by removing the sequence component separation from the controller stage. As discussed in the performance testing section, the proposed adaptive scheme yields an improved HVDC performance when contrasted with conventional controllers.

APPENDIX

In this Appendix the stability analysis of the proposed controller, taking into account the adaptation law dynamics, is carried out. Firstly, the Lyapunov candidate function below is considered

$$V = \frac{1}{2}\begin{bmatrix}\mathbf{e}\\ \mathbf{e}_p\end{bmatrix}^T \mathbf{P}\begin{bmatrix}\mathbf{e}\\ \mathbf{e}_p\end{bmatrix} \tag{26}$$

where the parameter error vector $\mathbf{e}_p$ is defined as

$$\mathbf{e}_p \triangleq \hat{\mathbf{p}} - \mathbf{p} = [e_R \quad e_L]^T = [\hat{R} - R \quad \hat{L} - L]^T \tag{27}$$

and the parameter vector as $\mathbf{p} \triangleq [R \quad L]^T$, being $\mathbf{P}$ the following positive-definite matrix:

$$\mathbf{P} \triangleq \begin{bmatrix}\mathbf{I} & \mathbf{0}\\ \mathbf{0} & |\frac{1}{L}|\gamma^{-1}\mathbf{I}\end{bmatrix} \tag{28}$$

where γ is a constant parameter of design. If the control law (17) is used with the correct parameters, the tracking error dynamics will be represented by (16). However, as the control law actually used is (18), with estimated parameters, the tracking error dynamics becomes

$$\dot{\mathbf{e}} = -a_d\mathbf{e} + \frac{1}{L}\left(\Omega_B\begin{bmatrix}e_R & e_L\\ -e_L & e_R\end{bmatrix}\mathbf{x} + e_L\mathbf{d}\right) \tag{29}$$

where $\mathbf{d} \triangleq \dot{\mathbf{x}}^d - a_d\mathbf{e}$.

The following adaptation law structure is proposed:

$$\dot{\hat{\mathbf{p}}} = -\text{sgn}\left(\frac{1}{L}\right)\gamma\mathbf{l}_a(\mathbf{x}, \mathbf{x}^d). \tag{30}$$

Then, taking the time derivative of the function V, and after some algebraic arrangement, the following is obtained:

$$\begin{aligned}\dot{V} &= \begin{bmatrix}\mathbf{e}\\ \mathbf{e}_p\end{bmatrix}^T\begin{bmatrix}\mathbf{I} & \mathbf{0}\\ \mathbf{0} & |\frac{1}{L}|\gamma^{-1}\mathbf{I}\end{bmatrix}\begin{bmatrix}\dot{\mathbf{e}}\\ \dot{\hat{\mathbf{p}}}\end{bmatrix},\\ &= -a_d\mathbf{e}^T\mathbf{e}\\ &\quad + \frac{\mathbf{e}^T\left(\Omega_B\begin{bmatrix}e_R & e_L\\ -e_L & e_R\end{bmatrix}\mathbf{x} + e_L\mathbf{d}\right) - \mathbf{e}_p^T\mathbf{l}_a(\cdot)}{L},\\ &= -a_d\mathbf{e}^T\mathbf{e}\\ &\quad + \frac{\mathbf{e}_p^T\begin{bmatrix}\Omega_B(e_1x_1 + e_2x_2)\\ \Omega_B(e_1x_2 - e_2x_1) + e_1d_1 + e_2d_2\end{bmatrix} - \mathbf{e}_p^T\mathbf{l}_a(\cdot)}{L}.\end{aligned} \tag{31}$$

Note that the second term in the above equation is a non-sign-defined term. In order to prove the tracking error stability, the function $\dot{V}$ must be a negative or seminegative definite function ($\dot{V} \leq 0$). Therefore, the second term of (31) is nullified by choosing

$$\mathbf{l}_a(\cdot) = \begin{bmatrix}\Omega_B(e_1x_1 + e_2x_2)\\ \Omega_B(e_1x_2 - e_2x_1) + e_1d_1 + e_2d_2\end{bmatrix}. \tag{32}$$

Replacing (32) into (30), the proposed adaptation laws (21) and (22) are obtained. Consequently, as mentioned above, considering (32) allows the following inequality to be verified:

$$\dot{V} = -a_d\mathbf{e}^T\mathbf{e} \leq 0. \tag{33}$$

This implies, from the Lyapunov stability theory, that the tracking error will be asymptotically stable ($\mathbf{e} \in \ell^2$), and the parameter estimation error remaining bounded ($\mathbf{e}_p \in \ell^\infty$).

REFERENCES

[1] L. Weimers, "HVDC light: A new technology for a better environment," *IEEE Power Eng. Rev.*, vol. 18, pp. 19–20, Aug. 1998.

[2] G. Asplund, K. Eriksson, and K. Svensson, "HVDC light—DC transmission based on voltage sourced converters," *ABB Rev.*, vol. 1, pp. 4–9, 1998.

[3] M. P. Bahrman and B. K. Johnson, "The ABCs of HVDC transmission technologies," *IEEE Power Energy Mag.*, vol. 5, pp. 32–44, Mar.–Apr 2007.

[4] N. Flourentzou, V. G. Agelidis, and G. D. Demetriades, "VSC-based HVDC power transmission systems: An overview," *IEEE Trans. Power Electron.*, vol. 24, pp. 592–602, Mar. 2009.

[5] B. Yin, R. Oruganti, S. K. Panda, and A. K. S. Bhat, "An output-power-control strategy for a three-phase PWM rectifier under unbalanced supply conditions," *IEEE Trans. Ind. Electron.*, vol. 55, pp. 2140–2151, May 2008.

[6] C. Hochgraf and R. H. Lasseter, "Statcom controls for operation with unbalanced voltages," *IEEE Trans. Power Del.*, vol. 13, pp. 538–544, Apr. 1998.

[7] H.-S. Song and K. Nam, "Dual current control scheme for PWM converter under unbalanced input voltage conditions," *IEEE Trans. Ind. Electron.*, vol. 46, pp. 953–959, Oct. 1999.

[8] A. Yazdani and R. Iravani, "A unified dynamic model and control for the voltage-sourced converter under unbalanced grid conditions," *IEEE Trans. Power Del.*, vol. 21, pp. 1620–1629, July 2006.

[9] Y. Suh, V. Tijeras, and T. A. Lipo, "A nonlinear control of the instantaneous power in dq synchronous frame for PWM AC/DC converter under generalized unbalanced operating conditions," in *Proc. 37th IAS Annu. Meet.*, Oct. 2002, vol. 2, pp. 1189–1196.

[10] F. A. Magueed, A. Sannino, and J. Svensson, "Transient performance of voltage source converter under unbalanced voltage dips," in *IEEE 35th Annu. Power Electron. Specialists Conf. (PESC'04)*, vol. 2, pp. 1163–1168.

[11] M. Bongiorno and J. Svensson, "Voltage dip mitigation using shunt-connected voltage source converter," *IEEE Trans. Power Electron.*, vol. 22, pp. 1867–1874, Sep. 2007.

[12] A. E. Leon, J. M. Mauricio, J. A. Solsona, and A. Gomez-Exposito, "Software sensor-based STATCOM control under unbalanced conditions," *IEEE Trans. Power Del.*, vol. 24, pp. 1623–1632, Jul. 2009.

[13] I. Etxeberria-Otadui, U. Viscarret, M. Caballero, A. Rufer, and S. Bacha, "New optimized PWM VSC control structures and strategies under unbalanced voltage transients," *IEEE Trans. Ind. Electron.*, vol. 54, pp. 2902–2914, Oct. 2007.

[14] R. Teodorescu, F. Blaabjerg, M. Liserre, and P. C. Loh, "Proportional-resonant controllers and filters for grid-connected voltage-source converters," *IEE Proc.—Electr. Power Appl.*, vol. 153, pp. 750–762, Sep. 2006.

[15] Y. Suh and T. A. Lipo, "Control scheme in hybrid synchronous stationary frame for PWM AC/DC converter under generalized unbalanced operating conditions," *IEEE Trans. Ind. Appl.*, vol. 42, pp. 825–835, May–Jun. 2006.

[16] Y. Suh and T. A. Lipo, "Modeling and analysis of instantaneous active and reactive power for PWM AC/DC converter under generalized unbalanced network," *IEEE Trans. Power Del.*, vol. 21, pp. 1530–1540, Jul. 2006.

[17] J. Hu and Y. He, "Modeling and control of grid-connected voltage-sourced converters under generalized unbalanced operation conditions," *IEEE Trans. Energy Convers.*, vol. 23, pp. 903–913, Sep. 2008.

[18] G. E. Valderrama, P. Mattavelli, and A. M. Stankovic, "Reactive power and imbalance compensation using STATCOM with dissipativity-based control," *IEEE Trans. Control Syst. Technol.*, vol. 9, pp. 718–727, Sep. 2001.

[19] G. Escobar, A. M. Stankovic, and P. Mattavelli, "An adaptive controller in stationary reference frame for D-statcom in unbalanced operation," *IEEE Trans. Ind. Electron.*, vol. 51, pp. 401–409, Apr. 2004.

[20] G. Escobar, P. Mattavelli, A. M. Stankovic, A. A. Valdez, and J. Leyva-Ramos, "An adaptive control for UPS to compensate unbalance and harmonic distortion using a combined capacitor/load current sensing," *IEEE Trans. Ind. Electron.*, vol. 54, pp. 839–847, Apr. 2007.

[21] A. Jain, K. Joshi, A. Behal, and N. Mohan, "Voltage regulation with STATCOMs: Modeling, control and results," *IEEE Trans. Power Del.*, vol. 21, pp. 726–735, Apr. 2006.

[22] Y. A.-R. I. Mohamed and E. F. El-Saadany, "An improved deadbeat current control scheme with a novel adaptive self-tuning load model for a three-phase PWM voltage-source inverter," *IEEE Trans. Ind. Electron.*, vol. 54, pp. 747–759, Apr. 2007.

[23] L. Yacoubi, K. Al-Haddad, L.-A. Dessaint, and F. Fnaiech, "A DSP-based implementation of a nonlinear model reference adaptive control for a three-phase three-level NPC boost rectifier prototype," *IEEE Trans. Power Electron.*, vol. 20, pp. 1084–1092, Sep. 2005.

[24] A. Allag, M. Y. Hammoudi, S. M. Mimoune, M. Y. Ayad, M. Becherif, E. Miliani, A. Miraoui, and M. Feliachi, "Adaptive nonlinear control applied to a three phase shunt active power filter," in *Proc. 32nd Annu. Conf. IEEE Ind. Electron. (IECON'06)*, pp. 1615–1620.

[25] B. Blazic and I. Papic, "Improved D-StatCom control for operation with unbalanced currents and voltages," *IEEE Trans. Power Del.*, vol. 21, pp. 225–233, Jan. 2006.

[26] M. K. Mishra, A. Ghosh, A. Joshi, and H. M. Suryawanshi, "A novel method of load compensation under unbalanced and distorted voltages," *IEEE Trans. Power Del.*, vol. 22, pp. 288–295, Jan. 2007.

[27] P. W. Lehn and M. R. Iravani, "Discrete time modeling and control of the voltage source converter for improved disturbance rejection," *IEEE Trans. Power Electron.*, vol. 14, pp. 1028–1036, Nov. 1999.

[28] P. Rioual, H. Pouliquen, and J.-P. Louis, "Regulation of a pwm rectifier in the unbalanced network state using a generalized model," *IEEE Trans. Power Electron.*, vol. 11, pp. 495–502, May 1996.

[29] K. Li, J. Liu, Z. Wang, and B. Wei, "Strategies and operating point optimization of STATCOM control for voltage unbalance mitigation in three-phase three-wire systems," *IEEE Trans. Power Del.*, vol. 22, pp. 413–422, Jan. 2007.

[30] Y. A.-R. I. Mohamed and E. F. El-Saadany, "A control scheme for PWM voltage-source distributed-generation inverters for fast load-voltage regulation and effective mitigation of unbalanced voltage disturbances," *IEEE Trans. Ind. Electron.*, vol. 55, pp. 2072–2084, May 2008.

[31] Z. Huang, B. T. Ooi, L.-A. Dessaint, and F. D. Galiana, "Exploiting voltage support of voltage-source HVDC," *IEE Proc. Gener, Transm. Distrib.*, vol. 150, pp. 252–256, Mar. 2003.

[32] S.-Y. Ruan, G.-J. Li, L. Peng, Y.-Z. Sun, and T. Lie, "A nonlinear control for enhancing HVDC light transmission system stability," *Int. J. Electr. Power Energy Syst.*, vol. 29, pp. 565–570, Sep. 2007.

[33] M. Torres, J. Espinoza, and R. Ortega, "Modeling and control of a high voltage direct current power transmission system based on active voltage source converters," in *Proc. 30th Annu. Conf. IEEE Ind. Electron. Soc. (IECON'04)*, vol. 1, pp. 816–821.

[34] J. L. Thomas, S. Poullain, and A. Benchaib, "Analysis of a robust DC-bus voltage control system for a VSC transmission scheme," in *Proc. 7th Int. Conf. AC-DC Power Transm.*, Nov. 2001, pp. 119–124.

[35] J. M. Mauricio and A. Goméz-Expósito, "Modeling and control of an HVDC-VSC transmission system," in *Proc. IEEE/PES Trans. Distrib. Conf. Expo.: Latin America (TDC'06)*, vol. 1, pp. 1–6.

[36] A. Yazdani and R. Iravani, "Dynamic model and control of the NPC-based back-to-back HVDC system," *IEEE Trans. Power Del.*, vol. 21, pp. 414–424, Jan. 2006.

[37] H. Chen, Z. Xu, and F. Zhang, "Nonlinear control for VSC based HVDC system," in *IEEE Power Eng. Soc. General Meet.*, 2006, pp. 1–5.

[38] F. A. R. Jowder and B. T. Ooi, "VSC-HVDC station with SSSC characteristics," *IEEE Trans. Power Electron.*, vol. 19, pp. 1053–1059, Jul. 2004.

[39] S. Filizadeh, A. M. Gole, D. A. Woodford, and G. D. Irwin, "An optimization-enabled electromagnetic transient simulation-based methodology for HVDC controller design," *IEEE Trans. Power Del.*, vol. 22, pp. 2559–2566, Oct. 2007.

[40] S.-Y. Ruan, G.-J. Li, X.-H. Jiao, Y.-Z. Sun, and T. Lie, "Adaptive control design for VSC-HVDC systems based on backstepping method," *Elect. Power Syst. Res.*, vol. 77, pp. 559–565, Apr. 2007.

[41] X. I. Koutiva, T. D. Vrionis, N. A. Vovos, and G. B. Giannakopoulos, "Optimal integration of an offshore wind farm to a weak AC grid," *IEEE Trans. Power Del.*, vol. 21, pp. 987–994, Apr. 2006.

[42] K. K. Y. Poon, Z. Lan, H. Zhu, and Y. Ni, "Application of a coordinated optimization algorithm for controller parameter tuning of HVDC power modulation control," *Proc. IEEE Power Eng. Soc. Gen. Meet.*, pp. 1–7, Jun. 2007.

[43] H. S. Ramadan, H. Siguerdidjane, and M. Petit, "A robust stabilizing nonlinear control design for VSC-HVDC systems: A comparative study," in *Proc. IEEE Int. Conf. Ind. Technol. (ICIT'09)*, pp. 1–6.

[44] J. E. R. Alves, L. A. S. Pilotto, and E. H. Watanabe, "An adaptive digital controller applied to HVDC transmission," *IEEE Trans. Power Del.*, vol. 8, pp. 1851–1859, Oct. 1993.

[45] C. Du, M. H. J. Bollen, E. Agneholm, and A. Sannino, "A new control strategy of a VSC-HVDC system for high-quality supply of industrial plants," *IEEE Trans. Power Del.*, vol. 22, pp. 2386–2394, Oct. 2007.

[46] C. Du, A. Sannino, and M. H. J. Bollen, "Analysis of response of VSC-based HVDC to unbalanced faults with different control systems," in *Proc. IEEE Transm. Distrib. Conf. Exhib.: Asia and Pacific*, 2005, pp. 1–6.

[47] J. Zhang, H. Chen, W. Pan, and C. Wangt, "VSC-HVDC control under unbalanced supply conditions," in *Proc. IEEE Power Eng. Soc. Gen. Meet.*, Jun. 2007, pp. 1–6.

[48] M. Hagiwara, K. Wada, H. Fujita, and H. Akagi, "Dynamic behavior of a 21-level BTB-based power-flow controller under single-line-to-ground fault conditions," *IEEE Trans. Ind. Appl.*, vol. 43, pp. 1379–1387, Sep.–Oct. 2007.

[49] L. Xu and V. G. Agelidis, "VSC transmission system using flying capacitor multilevel converters and hybrid PWM control," *IEEE Trans. Power Del.*, vol. 22, pp. 693–702, Jan. 2007.

[50] L. Xu, B. R. Andersen, and P. Cartwright, "VSC transmission operating under unbalanced AC conditions—Analysis and control design," *IEEE Trans. Power Del.*, vol. 20, pp. 427–434, Jan. 2005.

[51] H.-S. Song, I.-W. Joo, and K. Nam, "Source voltage sensorless estimation scheme for PWM rectifiers under unbalanced conditions," *IEEE Trans. Ind. Electron.*, vol. 50, pp. 1238–1245, Dec. 2003.

Andres E. Leon (S'05) was born in Argentina in 1979. He received the electrical engineering degree from the National University of Comahue, Neuquén, Argentina, in 2005. He is currently working toward his Ph.D. degree in control systems at the Instituto de Investigaciones en Ingeniería Eléctrica "Alfredo Desages" (IIIE), Universidad Nacional del Sur, Bahía Blanca, Argentina.

His primary areas of interest are power systems control, custom power systems, and wind energy conversion systems.

Juan Manuel Mauricio (M'01) was born in Argentina in 1977. He received the electrical engineering degree from the National University of Comahue, Neuquén, Argentina, in 2003 and the M.S. and Ph.D. degrees from the University of Seville, Spain, in 2007 and 2009, respectively.

Since 2004 he has been with the Department of Electrical Engineering, University of Seville, where he is currently an Assistant Professor. His primary areas of interest are power systems and electrical machines modeling and control, renewable energy generation, voltage source converters based applications, and electrical vehicles.

Jorge A. Solsona (SM'04) received the electronics engineer and Ph.D. degrees from the Universidad Nacional de La Plata, La Plata, Argentina, in 1986 and 1995, respectively.

Currently, he is with the Instituto de Investigaciones en Ingeniería Eléctrica Alfredo Desages (IIIE), Departamento de Ingeniería Eléctrica y de Computadoras, Universidad Nacional del Sur, Bahía Blanca, Argentina, and CONICET where he is involved in teaching and research on control theory and its applications to electromechanical systems.

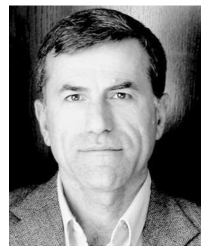

Antonio Gómez-Expósito (F'05) received the electrical engineering and Ph.D. degrees from the University of Seville, Spain.

Since 1982, he has been with the Department of Electrical Engineering, University of Seville, where he is currently a Professor and Chairman of the department. He is also directing the recently created Endesa Red Chair. His primary areas of interest are optimal power system operation, state estimation, digital signal processing, and control of flexible ac transmission system devices.